The Journal of Immunology

RESEARCH ARTICLE | JANUARY 15 2014

Regulatory T Cells Shape the Resident Memory T Cell Response to Virus Infection in the Tissues FREE

Jessica B. Graham; ... et. al

J Immunol (2014) 192 (2): 683–690.
https://doi.org/10.4049/jimmunol.1202153

Regulatory T Cells Shape the Resident Memory T Cell Response to Virus Infection in the Tissues

Jessica B. Graham,* Andreia Da Costa,*,† and Jennifer M. Lund*,†

Regulatory T cells (Tregs) are well known for their role in dampening the immune responses to self-Ags and, thereby, limiting autoimmunity. However, they also must permit immune responses to occur against foreign infectious agents. Using a mouse model of West Nile virus infection, we examined the role of Tregs in the generation of effector and memory T cell responses in the secondary lymphoid organs, as well as the infected tissues. We found that Treg numbers and activation increased in both the secondary lymphoid organs and CNS postinfection. Using Foxp3^{DTR} knock-in mice, we found that Treg-deficient mice had increased Ag-driven production of IFN-γ from both CD4$^+$ and CD8$^+$ T cells in the spleen and CNS during the effector phase. In mice lacking Tregs, there were greater numbers of short-lived effector CD8$^+$ T cells in the spleen during the peak of the immune response, but the memory CD8$^+$ T cell response was impaired. Specifically, we demonstrate that Treg-dependent production of TGF-β results in increased expression of CD103 on CD8$^+$ T cells, thereby allowing for a large pool of resident memory T cells to be maintained in the brain postinfection. *The Journal of Immunology*, **2014, 192: 683–690.**

Regulatory T cells (Tregs) are well known for their suppressive properties, which can reduce immune responses to self-Ags and prevent autoimmunity (1, 2). Recent work also highlighted the role of Tregs in the immune response to microbial infection (3). Several groups reported that Tregs limit vigorous immune responses that would assist in pathogen clearance at the expense of damaging healthy tissue (4). In some cases, this leads to a severely diminished effector T cell response that is unable to clear the infection adequately (5). Additionally, Tregs were shown to facilitate early immune responses to viral infection by coordinating a timely trafficking of lymphocytes to the infection site in an HSV-2 model (6). Thus, because Tregs have demonstrated roles in the suppression of, as well as the generation of, antimicrobial immunity, we hypothesized that Tregs could have distinct roles in antiviral immunity depending on the time postinfection, as well as the tissue microenvironment.

Thus, in this study, we used a well-established mouse model of West Nile virus (WNV) infection to investigate a role for Tregs in T cell responses to neurotropic virus infection at various times postinfection, as well as in various tissues. WNV is an ssRNA virus that cycles between mosquitos and birds, with humans and other mammals serving as incidental hosts. Approximately 20% of infected individuals experience a limited febrile illness, with 1% developing a more severe neuroinvasive disease characterized by encephalitis and meningitis (7). The immune response to WNV is known to involve both innate and adaptive responses, including humoral and cellular components. Upon infection in the skin following injection or mosquito bite, WNV replicates and is able to infect dendritic cells (DCs), including Langerhans cells, which can subsequently migrate to the draining lymph nodes (dLNs) where they initiate immune responses. DCs and other cells sense the presence of RNA virus infection through TLRs expressed within the endosomal compartment, as well as ubiquitously expressed cytoplasmic RNA sensors, such as *RIG-I* and *MDA-5* (8). One key immune mediator downstream of this virus-sensing mechanism is type I IFN, an important antiviral molecule capable of eliciting multiple antiviral pathways. Both T and B lymphocytes are involved in protection against WNV, and it was demonstrated in mouse studies that humoral immunity is involved in peripheral clearance of WNV, whereas T cells are critical for viral clearance within the CNS. Specifically, the induction of virus-specific IgM early postinfection with WNV limits viremia and spread to the CNS, thus helping to protect against lethal infection (9, 10). CTLs are also known to mediate immunity to WNV infection, because adoptive transfer of WNV-specific CD8$^+$ T cells results in a reduction of mortality and prolonged survival after WNV infection of recipient mice. CD8$^+$ T cells were found to infiltrate the infected brain, suggesting that they could be involved in recovery from encephalitis (11). CD4$^+$ T cell responses are also strongly induced and are required for the maturation of IgG responses, as well as sustaining CD8$^+$ T cell responses, both in the periphery and the CNS. Nevertheless, an absence of CD4$^+$ T cells did not cause a significant difference in viral titers in the periphery (12). WNV likely traffics from peripheral tissues to the CNS via axonal spread or by a hematogenous route across the blood–brain barrier (13). The generation of immune responses within the CNS are critical to clear the virus; however, at the same time, they must be regulated such that damage to nonrenewing populations of neurons is limited. Postinfection, CD8$^+$ T cells migrate to the brain, and their presence correlates with viral clearance (14). Indeed, in the absence of CD8$^+$ T cells, WNV persists in the brain of infected mice (15). Recruitment of T cells to the CNS is mediated by both CCL5 and CXCL10 (16–18). Although it was postulated that CD8$^+$ T cells may have a pathologic role in terms of damaging infected neurons, in addition to their protective role during WNV infection, it is

*Vaccine and Infectious Disease Division, Fred Hutchinson Cancer Research Center, Seattle, WA 98109; and †Graduate Program in Pathobiology, Department of Global Health, University of Washington, Seattle, WA 98195

Received for publication August 7, 2012. Accepted for publication November 15, 2013.

This work was supported by National Institutes of Health/National Institute of Allergy and Infectious Diseases Grants U19 AI083019 and R01 AI087657 (to J.M.L.).

Address correspondence and reprint requests to Dr. Jennifer M. Lund, Fred Hutchinson Cancer Research Center, 1100 Fairview Avenue N, E5-110, Seattle, WA 98109-1024. E-mail address: jlund@fhcrc.org

Abbreviations used in this article: DC, dendritic cell; dLN, draining lymph node; DT, diphtheria toxin; FHCRC, Fred Hutchinson Cancer Research Center; SLEC, short-lived effector cell; SLO, secondary lymphoid organ; Treg, regulatory T cell; T_{RM}, resident memory T cell; WNV, West Nile virus.

certainly clear that $CD8^+$ T cells are required for clearance of WNV from the CNS.

Studies (19, 20) in mice showed that WNV can persist in the periphery and CNS, despite the presence of virus-specific immune cells and Abs, for ≥16 wk postinfection. It is hypothesized that the virus might persist in certain tissues, such as the brain, for longer periods, as a result of the slow turnover of neuronal tissue and the need to limit immunopathology within the brain (21). Given the persistence of WNV in the CNS and the role of Tregs in balancing an adequate, but not overly robust, immune response, we sought to investigate how Tregs might modulate the effector and memory T cell response to virus infection in both the secondary lymphoid organs (SLOs), as well as the infected neuronal tissues. Further, because depletion of Tregs is known to result in increased WNV disease, weight loss, and lethality (22), we hypothesized that there would be dramatic effects on the T cell response to virus infection upon Treg depletion.

Our results show that Tregs limit Ag-driven proliferation of effector T cells in the CNS, as well as the production of inflammatory cytokines. In mice depleted of Tregs, there is an expansion of short-lived effector cells (SLECs) in the spleen at the peak of the effector phase, but the retention of Ag-specific $CD8^+$ T cells in the brain is impaired. Specifically, we found that Treg-dependent production of TGF-β leads to increased expression of CD103 on $CD8^+$ T cells, allowing a greater number of these resident memory T cells to remain in the brain postinfection. In sum, our study demonstrates the two-sided nature of Tregs; they can suppress but also potentiate the immune response to microbes, depending on the time postinfection, as well as the location within the host.

Materials and Methods

Virus

WNV TX-2002-HC was kindly provided by Dr. Michael Gale, Jr. (University of Washington) and propagated as previously described (23, 24). Working stocks were generated from supernatants collected from infected Vero cell lines and were stored at −80°C.

Mice and infection

C57BL/6 mice, 6–8 wk of age, were purchased from The Jackson Laboratory (Bar Harbor, ME) and housed in filtered cages. *Foxp3*^{DTR} (25) and *Foxp3*^{GFP} (26) mice (kindly provided by Dr. Alexander Rudensky, Memorial Sloan-Kettering Cancer Center, New York, NY) were bred onsite at the animal facility at the Fred Hutchinson Cancer Research Center (FHCRC). Age-matched 6–12-wk-old mice were inoculated s.c. in the left rear footpad with 100 PFU WNV TX-2002-HC. To ablate Tregs, *Foxp3*^{DTR} or *Foxp3*^{GFP} mice were treated i.p. with 30 μg/kg body weight of diphtheria toxin (DT) the day prior to infection and 10 μg/kg DT on the same day as infection. All animal experiments were approved by the FHCRC and the University of Washington Institutional Animal Care and Use Committee. The Office of Laboratory Animal Welfare of the National Institutes of Health approved the FHCRC's Animal Welfare Assurance (#A3226-01), as well as the University of Washington's Animal Welfare Assurance (#A3464-01), and this study was carried out in strict compliance with the Public Health Service Policy on Humane Care and Use of Laboratory Animals.

Cell preparation

Following euthanasia, mice were perfused with 10 ml PBS to remove any residual intravascular leukocytes. Popliteal dLNs were collected and processed to obtain single-cell suspensions. Spleens were homogenized, treated with ACK lysis buffer to remove RBCs, washed, and resuspended in FACS buffer (1× PBS, 2% FBS). To obtain lymphocytes from the CNS, brains were harvested into RPMI 1640, and a suspension was created through mechanical disruption. The suspension was added to hypertonic Percoll to create a 30% Percoll solution, vortexed, and centrifuged at 1250 rpm for 30 min at 4°C. After aspirating the supernatant, any remaining RBCs in the cell pellet were lysed with ACK, washed, passed through a 70-μm nylon mesh, and resuspended in FACS buffer. Cells were counted by a hemacytometer using trypan blue exclusion.

Flow cytometry analysis

Following preparation of single-cell suspensions, cells were plated at 1×10^6 cells/well and stained for surface markers for 15 min on ice. For tetramer staining, cells were stained with the WNV NS4b-$H2^d$ tetramer (generated by the Immune Monitoring Lab, FHCRC) for 30 min on ice. Cells were subsequently fixed, permeabilized (Foxp3 Fixation/Permeabilization Concentrate and Diluent; eBioscience), and stained with intracellular Abs for 30 min on ice. Cells from C57BL/6 mice were also stained with Foxp3-FITC at this time, as described previously (6). Flow cytometry was performed on a BD LSR II machine using BD FACSDiva software. Analysis was performed using FlowJo software.

The following directly conjugated Abs were obtained from eBioscience: CD4-PE (RM4-5) or PerCPCy5.5 (RM4-5), CD8-PECy5 (53-6.7), CTLA-4–PE (UC10-4B9), CD29-PE Cy7 (EbioHMb1-1), ICOS-PE (7E.17G9), CD62L-PerCPCy5.5 (MEL-14), CD127–Alexa Fluor 700 (A7R34), KLRG-1–PECy7 (2F1), IFN-γ PerCPCy5.5 (XMG1.2), TNF-α–allophycocyanin (MP6-XT22), CD103-PE (2E7), and Foxp3-FITC (FJK-16a). The Foxp3 Intracellular Staining kit (eBioscience) was used for fixation/permeabilization and all intracellular staining.

Intracellular cytokine staining

Splenocytes or CNS lymphocytes were resuspended at 1×10^6 cells/well in RPMI 1640 supplemented with 10% HI-FBS, 2.5 mM HEPES, 100 U/ml penicillin, 100 mg/ml streptomycin, 2 mM L-glutamine, and 1 mM sodium pyruvate to be analyzed for intracellular cytokine production. Lymphocytes were stimulated with one of four different stimulation mixtures: media, the WNV NS4b peptide (SSVWNATTAI), heat-inactivated WNV (multiplicity of infection = 5) or polyclonal stimulation using anti-CD3/CD28, and incubated for 5 h at 37°C. Cells were washed and stained with fixable viability stain (Fixable Viability Dye eFluor 780; eBioscience) for 30 min on ice, followed by surface staining for CD4-PE and CD8-PECy5 for 15 min on ice. The cells were then fixed, permeabilized, and stained with IFN-γ-PerCPCy5.5 and TNF-α–allophycocyanin, according to the manufacturer's protocol (eBioscience). After staining, the cells were analyzed as described above.

RNA extraction

Five brains/group were collected after whole-body perfusion with 10 ml cold PBS, snipped into pieces ~1 mm in thickness, and immediately placed into preweighed tubes containing 7 ml RNA*later* Stabilization Reagent (QIAGEN, Hilden, Germany). Samples were reweighed to determine the weight of brain alone and placed in a −80°C freezer. Brains were thawed at 4°C and homogenized using a handheld homogenizer, and total RNA was extracted following protocol instructions included with the RNeasy Lipid Tissue Midi Kit (QIAGEN). RNA was eluted into PCR-grade nuclease-free water, and RNA concentration was measured using a Nanodrop 2000 UV-Vis spectrophotometer (Thermo Scientific).

Quantitative RT-PCR for WNV RNA

Competent *Escherichia coli* cells, transformed with kanamycin-resistant plasmids containing the WNV PCR target region, were kindly provided by Dr. Michael Gale, Jr. (University of Washington). Cells were grown in kanamycin-containing media, and plasmids were isolated using the QIAGEN Plasmid Mini kit (QIAGEN). The plasmid concentration was determined using a Nanodrop 2000 UV-Vis spectrophotometer (Thermo Scientific), and a 10-fold standard dilution series was generated spanning a concentration of 1×10^{10} to 1×10^2 plasmids/5 μl.

WNV primers and probe were used as previously described (27). The fluorogenic probe was synthesized with a 5′ reporter dye FAM and a 3′ quencher dye TAMRA. Primers and probe were generated as custom assays from Integrated DNA Technologies (Coralville, Iowa). Quantitative RT-PCR assays were performed using the SuperScript III Platinum One-Step Quantitative RT-PCR System (Life Technologies, Grand Island, NY). Reactions were carried out in a total volume of 20 μl, containing 5 μl template RNA, 1× reaction mix, 500 nM final concentration for forward and reverse primers and 250 nM final concentration for probe, 0.4 μl ROX dye, and 0.4 μl RT/Taq polymerase enzyme mix and brought up with nuclease-free water. After adding the reaction mixture and template RNA to MicroAmp Fast Optical 96-Well Reaction Plates (Applied Biosystems, Foster City CA), reverse transcription and amplification were carried out on the ABI 7900 HT Fast Real-Time PCR System (Applied Biosystems) in standard mode. Cycling conditions were as follows: 50°C for 15-min hold (cDNA synthesis step), 95°C for 2-min hold, and 40 cycles of 95°C for 15 s followed by 60°C, for 1 min.

TGF-β ELISA

Whole-brain homogenates or purified samples of Tregs or conventional CD4 T cells were prepared and assayed for TGF-β by ELISA. Cell populations were isolated using the $CD4^+$ $CD25^+$ Regulatory T Cell Isolation kit (Miltenyi Biotec, Auburn, CA). Non-$CD4^+$ cells were indirectly magnetically labeled and depleted over a MACS column, and the flow-through fraction of pre-enriched $CD4^+$ T cells was labeled with CD25 MicroBeads for subsequent positive selection of $CD4^+CD25^+$ Tregs. Brain homogenates and purified cell populations were prepared and lysed using Nonidet P-40 lysis buffer containing complete protease inhibitor mixture tablets (Roche, Indianapolis, IN) for protein quantification. Lysates were centrifuged, and supernatants were stored at −80°C until the ELISA was performed according to the manufacturer's protocol (Mouse TGF-β ELISA kit; eBioscience). Briefly, samples were treated with acid and then neutralized to activate the latent TGF-β1 to the immunoreactive form. Standards and samples were incubated for 2 h at room temperature, followed by incubation with biotin and streptavidin-HRP. TMB substrate was used, and the plate was read by a spectrophotometer at 450 nm.

Statistical analysis

When comparing groups, two-tailed unpaired Student t tests were conducted, with p values < 0.05 considered significant. Error bars show ± SEM.

Results

Treg numbers increase and become activated in the dLNs and CNS after WNV infection

To determine whether Tregs respond to WNV infection, we first examined the kinetics and activation status of the Treg population following infection in both the footpad-draining popliteal lymph node and the brain. WNV infection was performed by s.c. injection in the rear footpad to mimic a mosquito bite, because WNV is a vector-borne viral infection. Importantly, $Foxp3^+$ Tregs were detectable in the brain postinfection, although they were largely absent in the naive brain (Fig. 1A), thereby demonstrating that Tregs are present and could play an important role in the immune response to WNV within the infected tissues. In the dLNs, Tregs expanded rapidly, beginning by day 4 postinfection and peaking around day 15, with total Treg numbers then decreasing through day 20. In the brain, Treg expansion occurred more gradually, with high numbers maintained out to a memory time point: day 60 postinfection (Fig. 1B). Treg expansion kinetics in the dLNs and brain were similar to those observed for the effector $CD4^+$ T cell population (data not shown). Likewise, activated effector T cell and Treg populations increased postinfection in both the dLN and brain, as indicated by increased expression of ICOS (Fig. 1C, data not shown). The frequency of CTLA-4^+ and $CXCR3^+$ Tregs also was increased in both the dLNs and brain (data not shown).

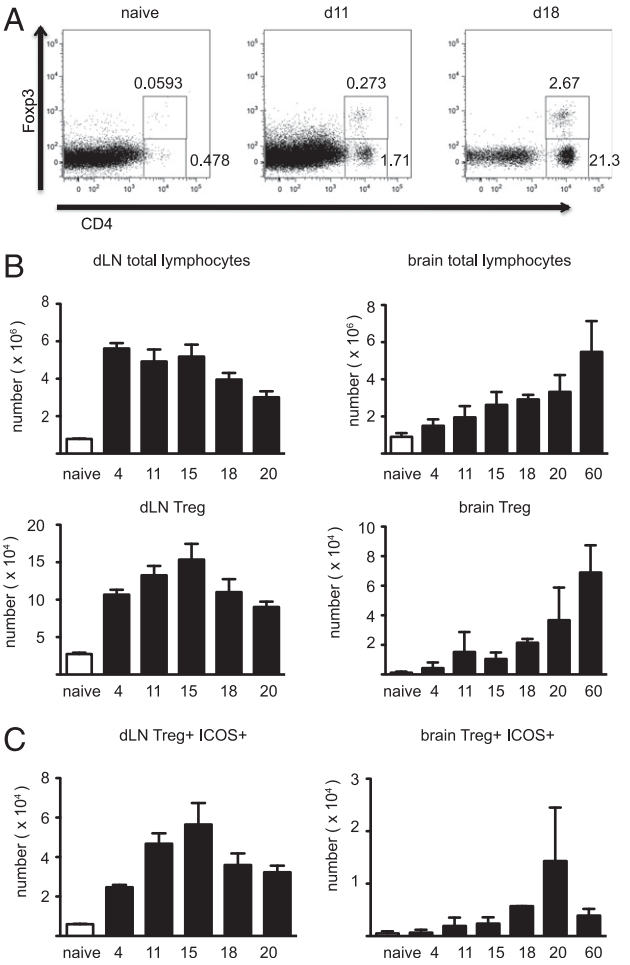

FIGURE 1. Treg numbers increase and become activated in the dLNs and CNS after WNV infection. *Foxp3^{gfp}* mice were inoculated s.c. in the footpad with 100 PFU WNV and sacrificed at the indicated time points postinfection. Data shown are representative of four to five mice/time point in three independent experiments. Error bars represent SEM. (**A**) Representative flow cytometric staining of CNS-derived lymphocytes for $CD4^+$ T cells and $CD4^+$ $Foxp3^+$ T cells at given time points postinfection. (**B**) Number of total lymphocytes (*top panels*) and Tregs (*bottom panels*) in the dLNs and brain from 0 to 60 d after WNV infection. (**C**) Number of $Treg^+$ $ICOS^+$ cells in the dLNs (*left panel*) or brain (*right panel*) at given time points after infection.

Tregs limit $CD4^+$ and $CD8^+$ T cell activation and infection-induced cytokine production

Because we observed Treg expansion and activation during WNV infection, we next examined the immune response in the systemic absence of Tregs using a mouse model of Treg ablation (25). *Foxp3^{GFP}* (26) and *Foxp3^{DTR}* mice were treated with DT on the day prior to and on the day of infection. The Treg population was successfully ablated in the *Foxp3^{DTR}* mice through early time points postinfection in the SLOs, as well as the brain, although, importantly, Treg frequency rebounded by day 14 postinfection in the SLOs and by day 20 postinfection in the brain (Fig. 2A). In Treg-deficient, WNV-infected mice, we observed increased numbers of activated $CD4^+$ and $CD8^+$ T cells in the dLNs and brain (Fig. 2B) compared with Treg-sufficient mice. These differences were most striking early postinfection—at day 4 postinfection in the dLNs and at days 8 and 11 postinfection in the brain—likely as a result of restoration of Treg homeostasis as DT is cleared from the host and Treg numbers return to steady state (Fig. 2A).

Because increased activation of T cells could be due merely to activation of bulk, non-WNV–specific cells in the absence of tight regulation by Tregs, we next determined the WNV-specific functionality of activated effector cells in the Treg-deficient mice in the context of infection. Twelve days postinfection, we performed intracellular cytokine staining to evaluate the number of $CD4^+$ and $CD8^+$ T cells that were producing IFN-γ, TNF-α, or both cytokines. The frequency of both $CD4^+$ and $CD8^+$ T cells producing IFN-γ directly in response to virus was increased in both the spleen and the brain of Treg-deficient mice, reaching statistical significance in the peripheral site of virus infection, the brain (Fig. 2C). Additionally, of the WNV-specific $CD4^+$ and $CD8^+$ T cells in both the SLOs and brain, Treg-ablated mice had an increased proportion of cells that were polyfunctional in their ability to produce both IFN-γ and TNF-α (Fig. 2D), likely leading to a more proinflammatory environment. In contrast, Treg-sufficient mice had more CD8 T cells producing IFN-γ or TNF-α alone, as

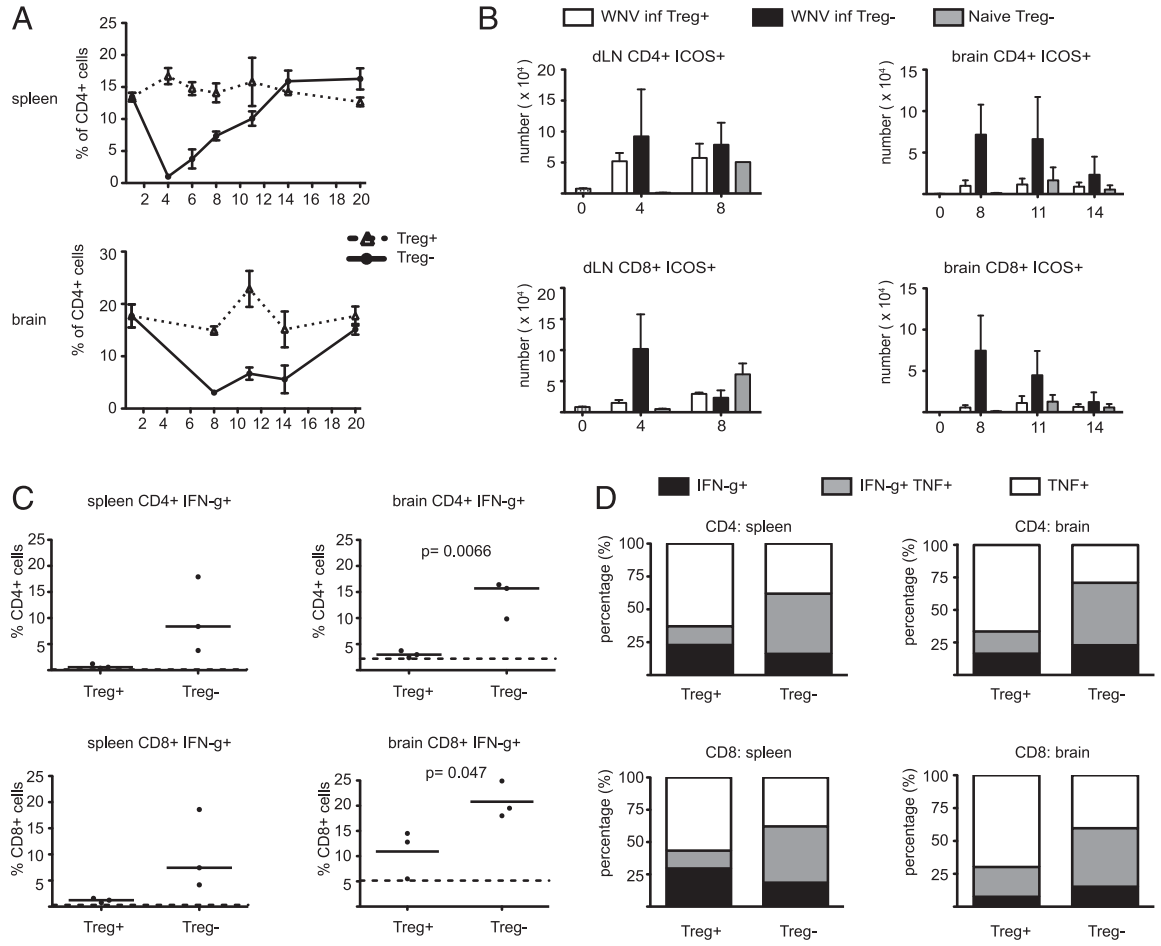

FIGURE 2. Treg depletion results in increased CD4 and CD8 T cell activation and infection-induced cytokine production. *Foxp3*^{DTR} mice (Treg$^-$) or *Foxp3*^{gfp} littermate controls (Treg$^+$) were treated with 30 μg/kg DT 1 d prior to infection and 10 μg/kg DT on the day of infection. WNV infection, or mock infection with PBS, was performed as described in the *Materials and Methods*. Data shown are from three to five mice/group for each time point and are representative of three independent experiments. Error bars represent SEM. (**A**) Frequency of Foxp3$^+$ Tregs following Treg depletion in splenocytes or CNS-derived lymphocytes in DT-treated *Foxp3*^{gfp} mice (Treg$^+$) or *Foxp3*^{DTR} mice (Treg$^-$) at the indicated days following WNV infection. (**B**) Number of CD4$^+$ ICOS$^+$ or CD8$^+$ ICOS$^+$ cells present in the dLNs at 4 or 8 d postinfection and in the brain at 8, 11, and 14 d postinfection in Treg-sufficient or -deficient mice. (**C**) Mean frequency of CD4$^+$ or CD8$^+$ T cells expressing IFN-γ following a 5-h stimulation with heat-inactivated WNV or NS4b peptide. Horizontal lines represent means for each group, and the dashed lines represent the DMSO control levels. (**D**) Frequency of single- or dual-cytokine producers (IFN-γ and TNF-α) in CD4$^+$ or CD8$^+$ T cells in the spleen and brain at day 12 postinfection.

was demonstrated by other investigators examining CD8 T cell functionality after WNV infection (Fig. 2D) (28–30). Finally, we quantified the levels of WNV present in the brain and spleen in Treg-sufficient or Treg-deficient mice. At day eight postinfection, there was no difference in WNV RNA in the spleen, regardless of the presence or absence of Tregs; further, there was no statistically significant difference at day 8 or 11 postinfection in the brain (Fig. 3), suggesting that the increased proinflammatory cytokine production observed in the brain upon Treg depletion is not due simply to enhanced virus replication upon Treg ablation.

Tregs modulate the fate of WNV-specific effector CD8 T cells in distinct tissue compartments

Because we observed differences in effector T cell activation and cytokine production during WNV infection in the absence of Tregs, we next considered how Tregs could affect the fate of WNV-specific T cells. To evaluate the effect of Treg ablation on the effector-to-memory cell transition in the context of WNV infection, we examined the frequency of WNV-specific CD8$^+$ T cells expressing the cell surface markers CD127 or KLRG-1 in Treg$^+$ or Treg$^-$ infected mice (31). Similar to results published previously using a vaccinia virus vector (32), ablation of Tregs resulted in increased numbers of SLECs, defined as CD127$^-$KLRG-1$^+$ tetramer$^+$ CD8$^+$ T cells, in the spleen 8 and 11 d post-WNV-infection (Fig. 4A, 4B). However, any difference observed in the number of SLECs present in the brain did not appear to be dependent on the presence of Tregs (Fig. 4A, 4B). We observed slightly elevated numbers of memory precursor effector cells, defined as tetramer$^+$ CD8$^+$ T cells that were CD127$^+$KLRG-1$^-$, in the spleen of Treg-sufficient mice 8 d postinfection, although this difference had disappeared by day 11 postinfection, and the numbers of memory precursor effector cells in the brain were equal, regardless of whether the mice had Tregs (Fig. 4A, 4B). Thus, the data suggest that Tregs can modulate the effector-to-memory T cell transition following virus infection in distinct ways, depending on the tissue microenvironment.

Tregs shape the generation of immunological memory to WNV

We next examined the kinetics of the WNV-specific CD8$^+$ T cell response out to day 60 postinfection in both the spleen and brain to determine how the memory T cell response is modulated by Tregs. In the spleen, we observed an expected peak in WNV-specific T cell numbers at day 12 postinfection that then declined by day 20 as the T cell population further contracted to

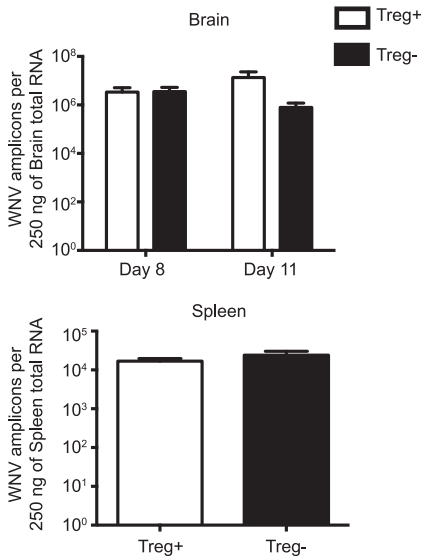

FIGURE 3. Quantification of WNV viral copy number. *Foxp3*^{DTR} mice (Treg$^-$) or *Foxp3*^{gfp} controls (Treg$^+$) were treated with 30 μg/kg DT 1 d prior to infection and 10 μg/kg DT on the day of infection. WNV infection was performed as described in the *Materials and Methods*. On days 8 and 11 postinfection, WNV copy numbers in the brains and spleens of infected Treg$^+$ or Treg$^-$ mice were measured by quantitative RT-PCR and expressed as WNV amplicons/250 ng of total RNA. Data shown are from four mice/group and are representative of three independent experiments. Error bars represent SEM.

a stable memory pool at day 60 postinfection. The pattern of CD8 T cell dynamics was similar, regardless of the presence or absence of Tregs, but Treg ablation resulted in an increase in the total number of Ag-specific CD8$^+$ T cells in the spleen at the peak of the effector phase (Fig. 4C). Strikingly, in the brain we observed that, in Treg-sufficient animals, there was a steady increase in WNV-specific CD8$^+$ T cells following infection out to a memory time point. In the absence of Tregs, there were similar numbers of Ag-specific CD8$^+$ T cells at the effector phase of the immune response (days 12 and 20 postinfection) compared with Treg-replete mice. However, in mice depleted of Tregs at the onset of virus infection, there were significantly fewer memory CD8$^+$ T cells present in the brain at day 60 postinfection, suggesting that Tregs are vital for the creation of memory T cells in the brain postinfection (Fig. 4C).

By virtue of time and location, it appears that the CD8$^+$ memory T cells present in the brain at day 60 postinfection are resident memory T cells (T_{RMs}). To further characterize the phenotype of these putative T_{RMs}, we examined the expression of CD103 on WNV-specific CD8$^+$ T cells in the brain at day 60 postinfection, because this integrin αE is known to be expressed by mucosal memory T cells and is suggested to be important for their retention in tissues, such as the intestinal epithelium, skin, and central nervous tissues (33). Furthermore, it was shown that CD103 expression phenotypically characterizes the majority of T_{RMs} in the CNS, and it also is important for their generation and accumulation (34). There were significantly fewer CD103$^+$ tetramer$^+$ CD8$^+$ T cells in the brain at day 60 in the absence of Tregs compared with in the presence of Tregs ($p = 0.0284$, Fig. 5), suggesting that Tregs are vital in the establishment of a T_{RM} population in the brain following WNV infection, as well as hinting at a mechanism by which Tregs could control recruitment and retention of these cells. Of note, WNV-infected Treg-deficient mice have a sizable population of tetramer$^-$ CD8 T cells in the brain that express CD103; however, because this population is similar in frequency to that observed in the brains of naive mice, we hypothesize that these are not WNV-specific T cells but rather are cells that are resident in the brain prior to infection with WNV (Fig. 5A).

Because the expression of CD103 is known to be positively regulated by TGF-β (33, 35), we next examined the levels of TGF-β protein in the brain at various times post-WNV infection. TGF-β levels were significantly lower in Treg-deficient mice 7 d postinfection compared with Treg-sufficient mice ($p = 0.0423$). Additionally, there was a trend for decreased TGF-β levels in Treg-deficient mice at days 9 and 12 post-WNV infection (Fig. 6A). Further, Tregs are a key cellular source of TGF-β in the brain after WNV infection because they contain significantly higher levels of TGF-β protein compared with conventional CD4 T cells ($p = 0.0003$, Fig. 6B). Therefore, we conclude that Tregs directly modulate the T_{RM} response to WNV in the brain via production of TGF-β.

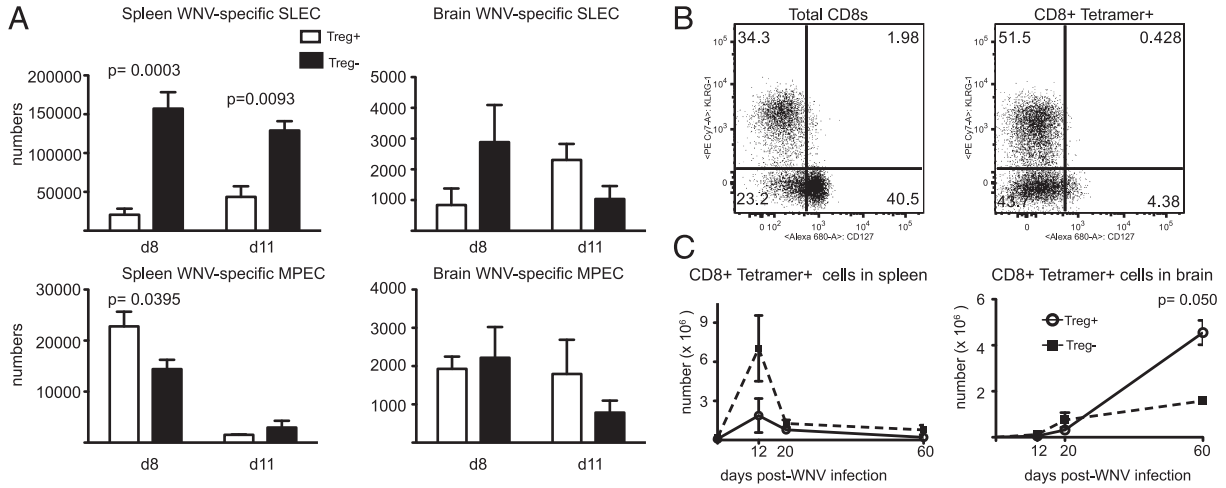

FIGURE 4. Tregs control the generation of virus-specific SLECs in lymphoid tissues and memory precursors in the infected tissues and shape the generation of immunological memory to WNV. *Foxp3*^{DTR} mice or *Foxp3*^{GFP} controls were treated with 30 μg/kg DT 1 d prior to WNV infection and 10 μg/kg DT on the day of infection. Data shown are from five mice/group and are representative of three to four independent experiments. Error bars represent ± SEM. (**A**) Eight or eleven days after WNV infection, mice were sacrificed, and lymphocytes from spleen and brain were prepared for flow cytometric analysis. Cells were gated on CD8 and MHC class I tetramer and further analyzed for markers of SLECs (KLRG-1$^+$CD127$^-$) or memory precursor cells (KLRG-1$^-$CD127$^+$). (**B**) Representative flow plots. (**C**) The numbers of CD8$^+$tetramer$^+$ cells in the spleen and brain at days 12, 20, and 60 postinfection.

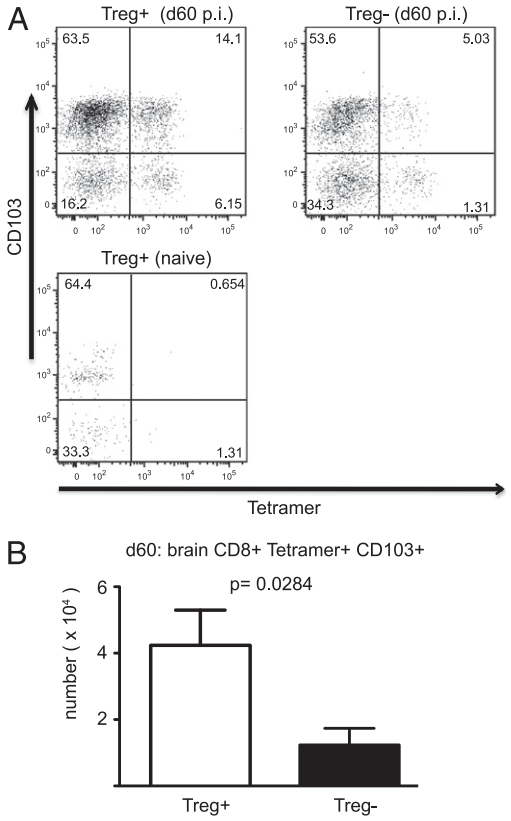

FIGURE 5. Tregs assist in the retention of resident memory T cells in the CNS. Treg-sufficient and -deficient mice were infected, as previously described, and tissues were harvested at day 60 and prepared for flow cytometry. (**A**) CNS-derived lymphocytes were gated on $CD8^+$ T cells. Flow cytometric plots show representative staining of the frequencies of virus-specific resident memory T cells ($tetramer^+CD103^+$) cells in each group of mice. (**B**) Mean numbers of resident memory T cells in the CNS. Data shown are from five mice/group for each time point and are representative of three independent experiments; error bars represent ± SEM.

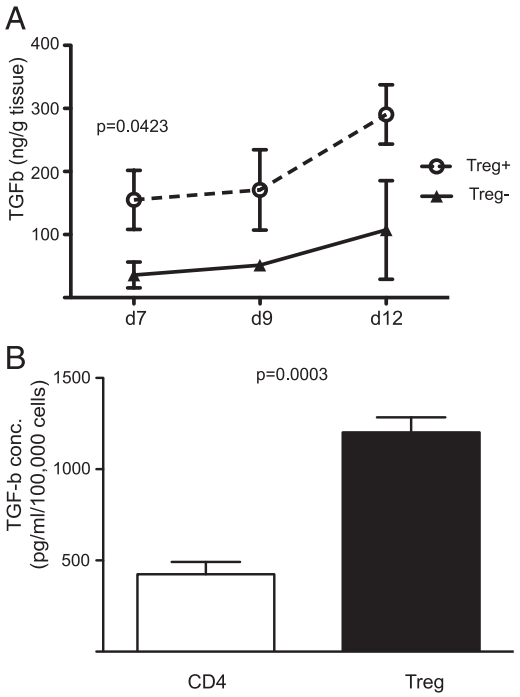

FIGURE 6. Treg-dependent production of TGF-β correlates with CD103 expression on T_{RMs} and subsequent retention in the CNS. (**A**) Treg-sufficient and -deficient mice were infected with 100 PFU WNV, and brains were harvested at days 7, 9, or 12 postinfection. CNS cell lysates were prepared, and TGF-β levels were measured by ELISA. Each sample was analyzed in duplicate, with five to seven mice/group for each time point. Error bars represent ± SEM. (**B**) *Foxp3*^{GFP} mice were infected with 100 PFU WNV, and brains were harvested 12 d postinfection. Single-cell suspensions of brains were used to prepare purified samples of Tregs or conventional CD4 T cells by MACS bead isolation, and cell lysates were subsequently prepared and assayed for TGF-β by ELISA.

Discussion

The generation of a robust antiviral immune response involves a rapid and dramatic clonal expansion of Ag-specific effector $CD4^+$ and $CD8^+$ T cells, which then contract to form a small, but potent, pool of stable memory T cells. In non-SLO tissues, it was shown that effector memory T cells are particularly poised for instant response to infection, because memory $CD8^+$ T cells from non-lymphoid tissues display effector levels of lytic activity directly ex vivo (36). Because it is known that circulating memory T cells do not access all tissues during immune surveillance, particularly the brain and intestinal lamina propria (37), the generation of T_{RM} populations may be of particular importance in these tissues. T_{RMs} are characterized as being tissue resident and self-renewing, as well as extremely protective against repeat infections. An elegant study of T_{RMs} in the brain by Wakim et al. (34) demonstrated that these cells express CD103, which was shown to be a phenotypic marker, as well as critical for their generation and accumulation. Further, Wakim et al. (34) demonstrated that brain T_{RMs} can persist in the absence of persistent antigenic stimulation, although they require local DC-dependent Ag presentation to upregulate CD103 on the incoming T cells.

During infection with WNV, a balance must exist between a robust immune response that clears the pathogen but limits destruction of nonrenewing populations of neurons in the brain. Given the role of Tregs in regulating and maintaining a delicate balance in immune responses to viral infections, we investigated the role of Tregs in the generation of effector and memory T cells both systemically and in the infected CNS. Using a mouse model in which Tregs could be ablated prior to infection, we showed that Treg-deficient mice had greater numbers of short-lived effector $CD8^+$ T cells in the spleen during the peak of the immune response, but the memory $CD8^+$ T cell response in the brain was impaired. Specifically, we demonstrate that Treg production of TGF-β results in increased expression of CD103 on $CD8^+$ T cells, thereby allowing for a large pool of resident memory T cells to be maintained in the brain postinfection. In our model of WNV infection in mice, as opposed to the work done by Wakim et al. (34) using intranasal infection with vesicular stomatitis virus, it is possible that there is prolonged Ag presentation in the brain, even after viral clearance, because Appler et al. (19) showed that WNV RNA persists in the CNS up to 3 mo postinfection. This prolonged Ag presentation could drive CD103 expression on T_{RMs}, perhaps through induction of Treg-dependent TGF-β production.

In the absence of Treg regulation during the immune response to viral infection, it is possible that bulk expansion of nonspecific CD4 and CD8 effector T cells contributes to the net increase in effector T cells observed in the CNS. However, we showed that Treg-deficient mice had increases in CD4 and CD8 cells specifically producing cytokine in response to WNV stimulation. Although these Treg-deficient mice had increased numbers of effector T cells and more robust cytokine production during the peak of infection, the number of memory T cells in the brain was significantly decreased compared with wild-type–infected mice at day 60 postinfection. This demonstrates that Tregs are vital for the creation of

memory T cells in the brain and that certain mechanisms and instructional cues must be in place to allow T cells to remain in such a tightly regulated area. Alternatively, it is possible that elimination of Tregs could impact the trafficking of CD8 T cells into the brain, which may explain the resultant differences that we observed in memory CD8 T cell numbers in the brain. Although this is possible, we favor the hypothesis that a lack of retention of CD8 T cells in the brain when Tregs are absent at the time of infection results in the deficit of T_{RMs}, because we note a decreased expression of CD103 on WNV-specific CD8 T cells in the brain upon Treg ablation (Fig. 5). Additionally, we did not observe a lack of WNV-specific CD8 T cells in the brain at early time points (Fig. 4A, 4C), suggesting that these cells are able to traffic to the CNS but fail to persist.

Our finding that Tregs control the generation of SLECs in the context of virus infection is similar to the findings by Kastenmuller et al. (32), who demonstrated that this was mechanistically due to a limited availability of IL-2, which is required for optimal SLEC generation. However, our results differ in that we uncovered a role for Tregs in the generation of immunological memory, likely due to the fact that we used a neurotropic virus capable of inducing $CD8^+$ T cell memory responses in the brain, pointing to the different roles that Tregs can play in immunity, depending on tissue location. Indeed, we speculate that the presence of Tregs during neurotropic virus infection can restrain $CD4^+$ and $CD8^+$ T cell production of proinflammatory and antiviral cytokines in the brain, thereby resulting in the incomplete viral clearance demonstrated by other investigators (19). This continued antigenic presence, in turn, could be important for sustained T_{RM} populations needed to protect the host from recurrent infections threatening this vital tissue. Recently, Casey et al. (38) demonstrated that TGF-β–driven CD103 expression was required for Ag-specific T_{RM} maintenance within the intestinal epithelium and, furthermore, that intestinal T_{RMs} were not dependent on prolonged cognate Ag stimulation. Our data similarly indicate that TGF-β–driven CD103 expression is likely required to allow T_{RMs} to persist in the brain; further, our work suggests a mechanism by which Tregs control and maintain the tissue-resident memory population.

In sum, our results suggest that Tregs are necessary to generate a pool of resident memory T cells, again highlighting the important role that these regulatory cells play in potentiating antiviral immunity. Although a significant population of T cells persisting in the brain could present a dangerous situation to the host, it is necessary to defend such critical tissues from neurotropic infection. Although we demonstrate that Tregs can negatively regulate T cell cytokine function in response to virus infection in the brain, they also play a pivotal role in establishing an appropriate T_{RM} population with which to protect the host from reinfection. Finally, the differing roles of Tregs in the SLOs compared with neuronal tissues suggest that the tissue microenvironment provides vital cues that play a significant role in defining T cell fates and balancing the host immune response to microbial infection.

Acknowledgments

We thank Steve Voght for critical reading of the manuscript, Greg Mize for expertise in RT-PCR techniques, and members of the Lund laboratory and the Center for the Study of Immune Mechanisms of Flavivirus Control (University of Washington) for helpful discussions. We also thank the James B. Pendleton Charitable Trust for their generous equipment donation.

Disclosures

The authors have no financial conflicts of interest.

References

1. Campbell, D. J., and M. A. Koch. 2011. Phenotypical and functional specialization of FOXP3+ regulatory T cells. *Nat. Rev. Immunol.* 11: 119–130.
2. Josefowicz, S. Z., L. F. Lu, and A. Y. Rudensky. 2012. Regulatory T cells: mechanisms of differentiation and function. *Annu. Rev. Immunol.* 30: 531–564.
3. Belkaid, Y., and K. Tarbell. 2009. Regulatory T cells in the control of host-microorganism interactions (*). *Annu. Rev. Immunol.* 27: 551–589.
4. Belkaid, Y., and B. T. Rouse. 2005. Natural regulatory T cells in infectious disease. *Nat. Immunol.* 6: 353–360.
5. Belkaid, Y., C. A. Piccirillo, S. Mendez, E. M. Shevach, and D. L. Sacks. 2002. CD4+CD25+ regulatory T cells control *Leishmania major* persistence and immunity. *Nature* 420: 502–507.
6. Lund, J. M., L. Hsing, T. T. Pham, and A. Y. Rudensky. 2008. Coordination of early protective immunity to viral infection by regulatory T cells. *Science* 320: 1220–1224.
7. Diamond, M. S., E. Mehlhop, T. Oliphant, and M. A. Samuel. 2009. The host immunologic response to West Nile encephalitis virus. *Front. Biosci. (Landmark Ed.)* 14: 3024–3034.
8. Kawai, T., and S. Akira. 2007. Antiviral signaling through pattern recognition receptors. *J. Biochem.* 141: 137–145.
9. Diamond, M. S., B. Shrestha, A. Marri, D. Mahan, and M. Engle. 2003. B cells and antibody play critical roles in the immediate defense of disseminated infection by West Nile encephalitis virus. *J. Virol.* 77: 2578–2586.
10. Diamond, M. S., E. M. Sitati, L. D. Friend, S. Higgs, B. Shrestha, and M. Engle. 2003. A critical role for induced IgM in the protection against West Nile virus infection. *J. Exp. Med.* 198: 1853–1862.
11. Wang, Y., M. Lobigs, E. Lee, A. Koskinen, and A. Müllbacher. 2006. CD8(+) T cell-mediated immune responses in West Nile virus (Sarafend strain) encephalitis are independent of gamma interferon. *J. Gen. Virol.* 87: 3599–3609.
12. Sitati, E. M., and M. S. Diamond. 2006. CD4+ T-cell responses are required for clearance of West Nile virus from the central nervous system. *J. Virol.* 80: 12060–12069.
13. Samuel, M. A., H. Wang, V. Siddharthan, J. D. Morrey, and M. S. Diamond. 2007. Axonal transport mediates West Nile virus entry into the central nervous system and induces acute flaccid paralysis. *Proc. Natl. Acad. Sci. USA* 104: 17140–17145.
14. Wang, T., E. Scully, Z. Yin, J. H. Kim, S. Wang, J. Yan, M. Mamula, J. F. Anderson, J. Craft, and E. Fikrig. 2003. IFN-gamma-producing gamma delta T cells help control murine West Nile virus infection. *J. Immunol.* 171: 2524–2531.
15. Shrestha, B., and M. S. Diamond. 2004. Role of CD8+ T cells in control of West Nile virus infection. *J. Virol.* 78: 8312–8321.
16. Glass, W. G., J. K. Lim, R. Cholera, A. G. Pletnev, J. L. Gao, and P. M. Murphy. 2005. Chemokine receptor CCR5 promotes leukocyte trafficking to the brain and survival in West Nile virus infection. *J. Exp. Med.* 202: 1087–1098.
17. Klein, R. S., E. Lin, B. Zhang, A. D. Luster, J. Tollett, M. A. Samuel, M. Engle, and M. S. Diamond. 2005. Neuronal CXCL10 directs CD8+ T-cell recruitment and control of West Nile virus encephalitis. *J. Virol.* 79: 11457–11466.
18. Shirato, K., T. Kimura, T. Mizutani, H. Kariwa, and I. Takashima. 2004. Different chemokine expression in lethal and non-lethal murine West Nile virus infection. *J. Med. Virol.* 74: 507–513.
19. Appler, K. K., A. N. Brown, B. S. Stewart, M. J. Behr, V. L. Demarest, S. J. Wong, and K. A. Bernard. 2010. Persistence of West Nile virus in the central nervous system and periphery of mice. *PLoS ONE* 5: e10649.
20. Stewart, B. S., V. L. Demarest, S. J. Wong, S. Green, and K. A. Bernard. 2011. Persistence of virus-specific immune responses in the central nervous system of mice after West Nile virus infection. *BMC Immunol.* 12: 6.
21. Garcia-Tapia, D., D. E. Hassett, W. J. Mitchell, Jr., G. C. Johnson, and S. B. Kleiboeker. 2007. West Nile virus encephalitis: sequential histopathological and immunological events in a murine model of infection. *J. Neurovirol.* 13: 130–138.
22. Lanteri, M. C., K. M. O'Brien, W. E. Purtha, M. J. Cameron, J. M. Lund, R. E. Owen, J. W. Heitman, B. Custer, D. F. Hirschkorn, L. H. Tobler, et al. 2009. Tregs control the development of symptomatic West Nile virus infection in humans and mice. *J. Clin. Invest.* 119: 3266–3277.
23. Keller, B. C., B. L. Fredericksen, M. A. Samuel, R. E. Mock, P. W. Mason, M. S. Diamond, and M. Gale, Jr. 2006. Resistance to alpha/beta interferon is a determinant of West Nile virus replication fitness and virulence. *J. Virol.* 80: 9424–9434.
24. Suthar, M. S., D. Y. Ma, S. Thomas, J. M. Lund, N. Zhang, S. Daffis, A. Y. Rudensky, M. J. Bevan, E. A. Clark, M. K. Kaja, et al. 2010. IPS-1 is essential for the control of West Nile virus infection and immunity. *PLoS Pathog.* 6: e1000757.
25. Kim, J. M., J. P. Rasmussen, and A. Y. Rudensky. 2007. Regulatory T cells prevent catastrophic autoimmunity throughout the lifespan of mice. *Nat. Immunol.* 8: 191–197.
26. Fontenot, J. D., J. P. Rasmussen, L. M. Williams, J. L. Dooley, A. G. Farr, and A. Y. Rudensky. 2005. Regulatory T cell lineage specification by the forkhead transcription factor foxp3. *Immunity* 22: 329–341.
27. Linke, S., H. Ellerbrok, M. Niedrig, A. Nitsche, and G. Pauli. 2007. Detection of West Nile virus lineages 1 and 2 by real-time PCR. *J. Virol. Methods* 146: 355–358.
28. Suthar, M. S., H. J. Ramos, M. M. Brassil, J. Netland, C. P. Chappell, G. Blahnik, A. McMillan, M. S. Diamond, E. A. Clark, M. J. Bevan, and M. Gale, Jr. 2012. The RIG-I-like receptor LGP2 controls CD8(+) T cell survival and fitness. *Immunity* 37: 235–248.

29. Ma, D. Y., M. S. Suthar, S. Kasahara, M. Gale, Jr., and E. A. Clark. 2013. CD22 is required for protection against West Nile virus Infection. *J. Virol.* 87: 3361–3375.
30. Ramos, H. J., M. C. Lanteri, G. Blahnik, A. Negash, M. S. Suthar, M. M. Brassil, K. Sodhi, P. M. Treuting, M. P. Busch, P. J. Norris, and M. Gale, Jr. 2012. IL-1β signaling promotes CNS-intrinsic immune control of West Nile virus infection. *PLoS Pathog.* 8: e1003039.
31. Cui, W., and S. M. Kaech. 2010. Generation of effector CD8+ T cells and their conversion to memory T cells. *Immunol. Rev.* 236: 151–166.
32. Kastenmuller, W., G. Gasteiger, N. Subramanian, T. Sparwasser, D. H. Busch, Y. Belkaid, I. Drexler, and R. N. Germain. 2011. Regulatory T cells selectively control CD8+ T cell effector pool size via IL-2 restriction. *J. Immunol.* 187: 3186–3197.
33. Sheridan, B. S., and L. Lefrançois. 2011. Regional and mucosal memory T cells. *Nat. Immunol.* 12: 485–491.
34. Wakim, L. M., A. Woodward-Davis, and M. J. Bevan. 2010. Memory T cells persisting within the brain after local infection show functional adaptations to their tissue of residence. *Proc. Natl. Acad. Sci. USA* 107: 17872–17879.
35. Robinson, P. W., S. J. Green, C. Carter, J. Coadwell, and P. J. Kilshaw. 2001. Studies on transcriptional regulation of the mucosal T-cell integrin alphaEbeta7 (CD103). *Immunology* 103: 146–154.
36. Masopust, D., V. Vezys, A. L. Marzo, and L. Lefrançois. 2001. Preferential localization of effector memory cells in nonlymphoid tissue. *Science* 291: 2413–2417.
37. Klonowski, K. D., K. J. Williams, A. L. Marzo, D. A. Blair, E. G. Lingenheld, and L. Lefrançois. 2004. Dynamics of blood-borne CD8 memory T cell migration in vivo. *Immunity* 20: 551–562.
38. Casey, K. A., K. A. Fraser, J. M. Schenkel, A. Moran, M. C. Abt, L. K. Beura, P. J. Lucas, D. Artis, E. J. Wherry, K. Hogquist, et al. 2012. Antigen-independent differentiation and maintenance of effector-like resident memory T cells in tissues. *J. Immunol.* 188: 4866–4875.